Published online: February 12, 2018

Article

SOURCE DATA | TRANSPARENT PROCESS

THE EMBO JOURNAL

IRES-mediated translation of cofilin regulates axonal growth cone extension and turning

Jung-Hyun Choi[1], Wei Wang[2,3,†], Dongkeun Park[2,3], Sung-Hoon Kim[4,‡], Kyong-Tai Kim[1,4,*] & Kyung-Tai Min[2,3,**]

Abstract

In neuronal development, dynamic rearrangement of actin promotes axonal growth cone extension, and spatiotemporal translation of local mRNAs in response to guidance cues directs axonal growth cone steering, where cofilin plays a critical role. While regulation of cofilin activity is well studied, regulatory mechanism for cofilin mRNA translation in neurons is unknown. In eukaryotic cells, proteins can be synthesized by cap-dependent or cap-independent mechanism via internal ribosome entry site (IRES)-mediated translation. IRES-mediated translation has been reported in various pathophysiological conditions, but its role in normal physiological environment is poorly understood. Here, we report that 5′UTR of *cofilin* mRNA contains an IRES element, and cofilin is predominantly translated by IRES-mediated mechanism in neurons. Furthermore, we show that IRES-mediated translation of cofilin is required for both axon extension and axonal growth cone steering. Our results provide new insights into the function of IRES-mediated translation in neuronal development.

Keywords axonal growth cone; cofilin; internal ribosome entry sites
Subject Categories Neuroscience; Protein Biosynthesis & Quality Control; RNA Biology
DOI 10.15252/embj.201695266 | Received 18 July 2016 | Revised 19 December 2017 | Accepted 5 January 2018 | Published online 12 February 2018
The EMBO Journal (2018) 37: e95266

Introduction

During brain development, axonal growth cones navigate toward their targets to establish synapses, which is crucial for brain wiring and its functions (Buck & Zheng, 2002; Dent *et al*, 2011; Vitriol & Zheng, 2012). In axonal growth cones, cytoskeleton dynamics including coordinated reorganization of actin polymerization is essential for axon extension and axonal growth cone guidance (Dent *et al*, 1999; Schaefer *et al*, 2008; Lowery & Van Vactor, 2009). Furthermore, cofilin, an actin-binding protein, plays a key role in regulating actin dynamics. Cofilin binds to F-actin and severs actin filaments, which controls actin polymerization as well as depolymerization (Bamburg & Bernstein, 2010; Pfaendtner *et al*, 2010; Grintsevich *et al*, 2016). Thus, regulation of cofilin activity is critical in axon extension and axonal growth cone steering (Aizawa *et al*, 2001; Hsieh *et al*, 2006; Piper *et al*, 2006; Tilve *et al*, 2015). It is proposed that LIM kinases deactivate cofilin by phosphorylation, which provides a fine balance between active and inactive cofilin that determines axonal growth cone extension and navigation (Arber *et al*, 1998; Aizawa *et al*, 2001). A large number of studies have described how the balance of cofilin activity is controlled and how the cofilin regulation affects axonal growth cone development (Gehler *et al*, 2004; Chen *et al*, 2006; Tilve *et al*, 2015; Bellon *et al*, 2017). However, a regulatory mechanism for *cofilin* mRNA translation in neurons remains unknown.

In eukaryotes, initiation of mRNA translation mechanism requires ribosomes to recognize a 5′ end cap structure of mRNAs, followed by scanning the mRNA transcripts. In addition to the cap-dependent translation, noncanonical translation initiation is discovered in picornaviruses, which contain internal ribosome entry sites (IRES) located in the 5′UTR of mRNAs that can directly recruit ribosomes to initiate translation without scanning from the 5′ end of mRNAs (Pelletier & Sonenberg, 1988; Kieft, 2008; Martinez-Salas, 2008; Hinnebusch *et al*, 2016). Since the initial discovery of IRES in picornaviruses, IRES-mediated translation has been identified in many RNA and DNA viruses (Ray & Das, 2002; Zhang *et al*, 2015). Furthermore, numerous reports show that eukaryotic mRNAs are also translated by IRES-mediated mechanisms under various stressful environments, when canonical translation is altered (Graber & Holcik, 2007; Kim *et al*, 2013, 2015; Olson *et al*, 2013; Shi *et al*, 2016). It suggests that eukaryotes adopt an alternative translation mechanism to compensate for the defective cap-dependent translation. However, physiological importance of IRES-mediated translation in nonpathological conditions has just begun to emerge (Pinkstaff *et al*, 2001;

1 Department of Life Sciences, Pohang University of Science and Technology, Pohang, Korea
2 Department of Biological Sciences, School of Life Sciences, Ulsan, Korea
3 National Creative Research Initiative Center for Proteostasis, Ulsan National Institute of Science and Technology, Ulsan, Korea
4 Division of Integrative Biosciences and Biotechnology, Pohang University of Science and Technology, Pohang, Korea
*Corresponding author. Tel: +82 54 279 2297; E-mail: ktk@postech.ac.kr
**Corresponding author. Tel: +82 52 217 5202; E-mail: ktaimin@unist.ac.kr
†The School of Mental Health, Wen Zhou Medical University, Wen Zhou, Zhejiang Province, China
‡Department of Biochemistry and Goodman Cancer Research Centre, McGill University, Montreal, QC, Canada

Fernandez *et al*, 2002; Audigier *et al*, 2008; Yeh *et al*, 2011; Lee *et al*, 2014; Liu, 2015). While there are few studies reporting cellular mRNA IRES in the brain, IRES-mediated translation has recently been shown to play a key regulatory role during mammalian development (Audigier *et al*, 2008; Srivastava *et al*, 2012; Xue *et al*, 2015). Also, high-throughput screening for IRES elements in human genomes identified that about 10% of human 5′UTR contain IRES element (Weingarten-Gabbay *et al*, 2016; Gritsenko *et al*, 2017), suggesting that IRES-mediated translation may be essential for normal biological functions. Nonetheless, physiological functions of IRES-mediated translation remain to be discovered.

While screening for neuronal genes that have IRES activity, we discovered that the 5′UTR of *cofilin* mRNA contains IRES element. In this work, we report that the 5′UTR of *cofilin* contains IRES activity in axonal growth cones and that reducing IRES activity of *cofilin* 5′UTR results in decreased axonal growth cone extension and loss of repulsion to Sema3A. Our study reveals that *cofilin* 5′UTR prefers IRES-mediated translation to cap-dependent translation in neurons. Disrupting IRES activity using CRISPR–Cas9 system in Neuro2A cells abolished cofilin expression, confirming that cofilin is generated mostly by IRES-mediated translation mechanism in neurons. Furthermore, we demonstrate that nPTB plays as ITAF for IRES-mediated cofilin translation. Our work provides an important step toward understanding the physiological significance of IRES-mediated translation in axon outgrowth and axonal growth cone navigation during neuronal development. IRES-mediated translation mechanism could shed new insights into cellular and molecular mechanisms of protein synthesis in diverse physiological conditions.

Results

Cofilin 5′UTR contains IRES activity

To demonstrate whether cofilin expression in neurons utilizes IRES-mediated translation, we first determined whether 5′UTR of *cofilin* harbors IRES activity by using a bicistronic reporter system (Kim *et al*, 2007), which can distinguish cap-dependent (*renilla luciferase*, RLUC) and cap-independent (*firefly luciferase*, FLUC) translation. *Cofilin* 5′UTR was inserted between the two reporters, and the ratio of FLUC/RLUC was measured in Neuro2A cells. *Cofilin* 5′UTR showed profound IRES activity compared to those of controls which contain reversely oriented *cofilin* 5′UTR or no insertion into the reporter system (Fig 1A). We also monitored *Apaf-1* 5′UTR IRES activity as control (Fig 1A), which indeed showed IRES activity consistent with a previous report (Mitchell *et al*, 2003). To further confirm that *cofilin* 5′UTR contains IRES activity, we also (i) examined the reporter containing *cofilin* 5′UTR with or without CMV promoter (Fig 1B); (ii) tested the integrity of our constructs using siRNA against RLUC and then measured RLUC and FLUC activity (Fig 1C and D); and (iii) used mRNA transcripts of the bicistronic reporters containing either *cofilin* 5′UTR or cofilin 5′UTR lacking D1 loop (Δ1–34) (Fig 1G), which were prepared by *in vitro* transcription. Together, these results demonstrate that *cofilin* 5′UTR indeed contains IRES activity.

It is known that the RNA secondary structure of IRES is important for IRES function (Martineau *et al*, 2004; Filbin & Kieft, 2009; Colussi *et al*, 2015). Hence, to determine the RNA domain that is responsible for IRES activity, we first generated a predicted secondary structure of the 5′UTR RNA of *cofilin* by using mfold software (Zuker, 2003), which showed three different regions containing loop domains (Fig 1E). We then deleted each of these regions (D1, D2, and D3) in the 5′UTR sequence (Appendix Fig S1) and examined IRES activity of the sequences (Fig 1F). Absence of D1 (Δ1–34) significantly decreased IRES activity, while D2 (Δ62–84) and D3 (Δ91–111) deletion still displayed limited IRES activity. However, removing D2 or D3 combined with D1 deletion completely abolished IRES activity, suggesting that the D1 region is absolutely required for IRES activity in *cofilin* 5′UTR. To further verify the importance of the loop in D1 for IRES activity, we mutated nucleotides that disrupt the loop formation (Appendix Fig S1B). Either deleting the D1 region or disrupting formation of the loop in D1 blocked IRES activity (Appendix Fig S1C), which confirms that the loop in D1 is required for IRES activity of *cofilin* 5′UTR. Lastly, to exclude the possibility

Figure 1. 5′UTR of *cofilin* harbors IRES activity.

A 5′UTR of *cofilin* shows strong IRES activity, while reversely oriented 5′UTR of *cofilin* lacks IRES activity. This was measured by using a bicistronic reporter system. Cap-dependent (*renilla luciferase*, RLUC) and cap-independent (*firefly luciferase*, FLUC) translation can be distinguished by determining the ratio of FLUC to RLUC. FLUC cannot be synthesized unless DNA fragment inserted into the intercistronic region contains IRES activity. FLUC and RLUC activities were normalized to β-galactosidase activity, which is used as an independent transfection control. For IRES activity measurement, Neuro2A cells were transfected with pRF (backbone of bicistronic reporter system), pRF containing 5′UTR of *cofilin* (5′UTR), or reversely oriented 5′UTR of *cofilin* (R-5′UTR). *$P < 0.0001$, $N = 5$ independent experiments. Values shown are mean ± SEM and are tested for statistical significance by one-way ANOVA followed by Bonferroni *post hoc* test.

B Both pCMV-β-gal vector and pRF (backbone of bicistronic reporter system) containing 5′UTR of *cofilin* (5′UTR) or 5′UTR lacking a CMV promoter (ΔCMV) were transfected into Neuro2A cells, and dual-luciferase assays were performed. FLUC and RLUC activities were normalized to β-galactosidase activity. $N = 3$ independent experiments. Values shown are mean ± SEM.

C, D pCMV-β-gal vector and the indicated plasmids were co-transfected with siRNA targeting *RLUC*. After 48-h transfection, Neuro2A cell lysates were used for measuring luciferase activity. FLUC and RLUC activities were normalized to β-galactosidase activity. *RLUC* siRNA reduced RLUC but not FLUC in cells transfected with psi-Check2 (control). While *RLUC* siRNA significantly decreased RLUC, FLUC still exhibited strong activity in cells transfected with *cofilin* 5′UTR. *Apaf-1* 5′UTR also showed FLUC activity compared to that of *cofilin* R-5′UTR. Note that *Apaf-1* IRES activity is significantly lower than that of cofilin. $N = 3$. Values shown are mean ± SEM and are tested for statistical significance by one-way ANOVA followed by Bonferroni *post hoc* test.

E A secondary structure of 5′UTR of *cofilin* having 145 nucleotides was prepared with mfold software, which produced three different regions containing loop domains. Deletion of nucleotides (Δ1–34, Δ62–84, or Δ91–111) removed the D1, D2, or D3 loop, respectively. Also, deletion of D1 together with D2 (Δ1–84) or all loops including D1, D2, and D3 (Δ1–92) was generated.

F RLUC and FLUC activities were measured with different mutations of *cofilin* 5′UTR. $N = 5$. Values shown are mean ± SEM.

G Bicistronic mRNA transcripts prepared by *in vitro* transcription were transfected into Neuro2A cells and incubated for 24 h, and then, IRES activity was measured. Values are normalized to the cells containing mRNA transcripts prepared from pRF vector used in (A and E). m^7G: 7-methyl-guanosine. *$P < 0.0001$, $N = 4$. Values shown are mean ± SEM and are tested by one-way ANOVA followed by Bonferroni *post hoc* test.

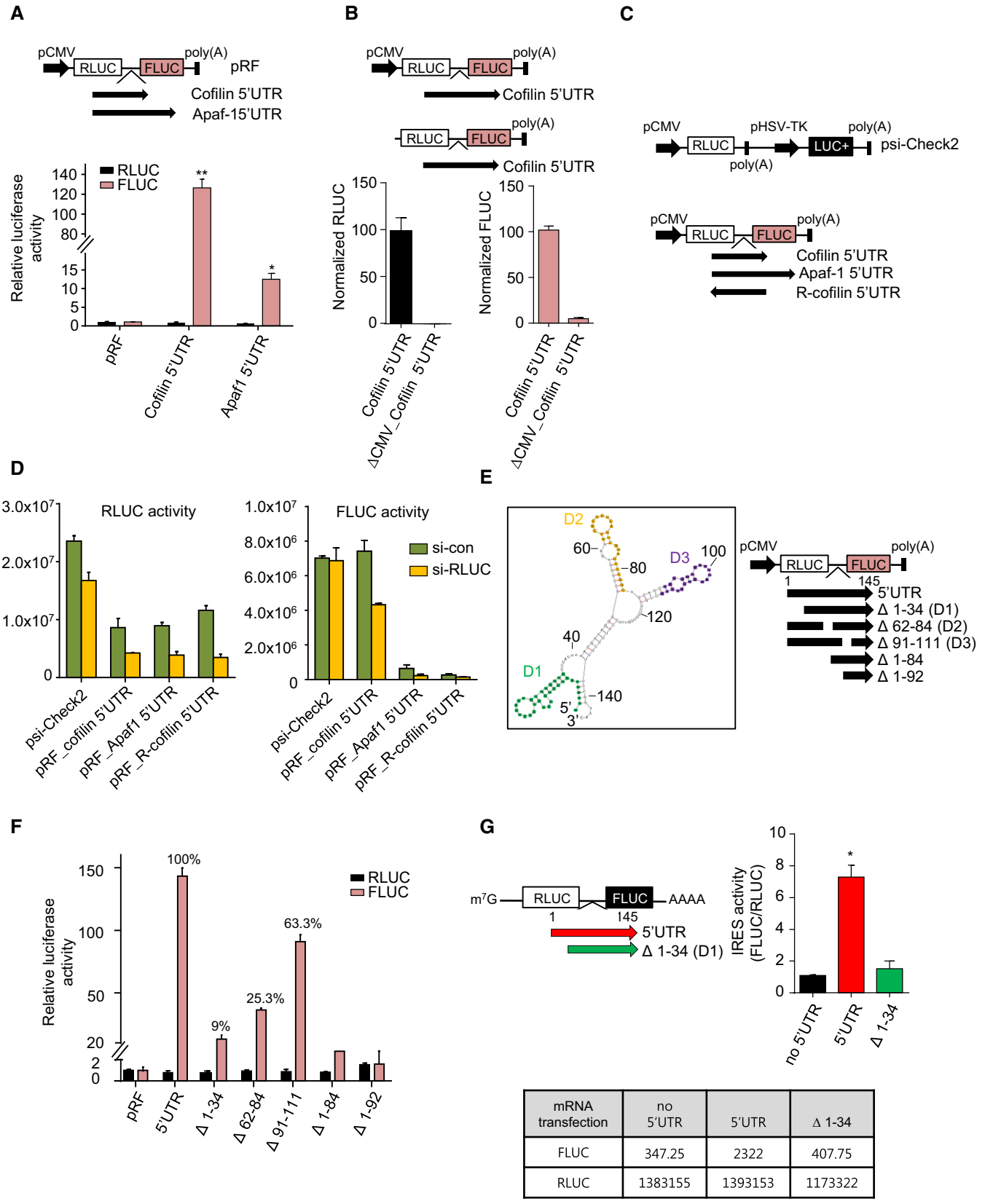

mRNA transfection	no 5'UTR	5'UTR	Δ 1-34
FLUC	347.25	2322	407.75
RLUC	1383155	1393153	1173322

Figure 1.

that a cryptic promoter may be hidden in *cofilin* 5′UTR, we performed real-time quantitative PCR for *RLUC* and *FLUC* mRNA transcripts from the vectors that we used in Appendix Fig S1C. The ratio of *FLUC/RLUC* mRNA transcripts is equivalent among the vectors regardless of IRES activity, indicating that no cryptic promoter activity exists in *cofilin* 5′UTR (Appendix Fig S1D).

Cofilin expression by IRES-mediated translation promotes axon outgrowth

Because cofilin plays a key role in axonal growth cone extension (Yoon *et al*, 2012) and *cofilin* 5′UTR harbors an IRES element, we hypothesized that *cofilin* mRNA is translated by IRES-mediated mechanism in axonal growth cones. To test this hypothesis, we first constructed a plasmid in which RLUC and FLUC reporters were replaced with mCherry and eGFP fluorescent reporters in the bicistronic reporter system. The reporter plasmid was then transfected to mouse primary hippocampal neurons at DIV1, and axonal growth cones at DIV3 was examined (Fig 2A). eGFP signals originating from IRES-mediated translation were examined in axonal growth cones at DIV3 (Fig 2A and B). Axonal growth cones containing *cofilin* 5′UTR-*eGFP* clearly showed IRES activity, while growth cones having reversely oriented *cofilin* 5′UTR or lacking the D1 region in *cofilin* 5′UTR exhibited no IRES activity (Fig 2A and B). Together, these results suggest that *cofilin* 5′UTR utilizes its IRES element to express eGFP, and *cofilin* mRNA may be translated by IRES-mediated translation in axonal growth cones.

Having confirmed that *cofilin* 5′UTR has IRES activity in neurons, we next examined the functional role of IRES-mediated *cofilin* translation. When the cofilin protein was expressed by introducing 5′UTR-*cofilin-eGFP* construct to primary hippocampal neurons, axon length of the neurons was significantly increased compared to that of axons containing either 5′UTR(ΔD1)-*cofilin-eGFP* or no 5′UTR of *cofilin* (Fig 2C and D). Consistent with these results, axonal growth cones containing 5′UTR-*cofilin-eGFP* construct showed faster axonal growth rate and longer traveled distance during the 60-min observation period than axonal growth cones with 5′UTR(Δ1–34)-*cofilin-eGFP* (Appendix Fig S2). These data suggest that cofilin overexpression due to IRES-mediated translation provides further extension of axonal growth cones. Note that no change was found in the ratio of *mCherry/eGFP* mRNA transcripts in primary neurons containing different plasmids used above (Fig 2E).

Cofilin is preferentially expressed by IRES-mediated translation

We found that cofilin expression by IRES-mediated translation in neurons extended axonal growth cones. Next, we tested whether newly synthesized cofilin in neurons exploited IRES-mediated translation mechanism. To this end, we first prepare a vector that was designed to express the FLAG peptide under the control of either *cofilin* 5′UTR (*cofilin*-5′UTR-*FLAG*) or *cofilin* 5′UTR lacking the D1 region [*cofilin*-5′UTR (Δ1–34)-*FLAG*] (Fig 3A). To determine whether FLAG is newly synthesized by IRES-mediated mechanism in hippocampal neurons, we used the FUNCAT-PLA (fluorescent noncanonical amino acid tagging–proximity ligation assay) method that allows visualization of a newly synthesized protein *in situ* (tom Dieck *et al*, 2015). IRES-mediated translation of *FLAG* mRNAs (*cofilin* 5′UTR-*FLAG*) was detected by proximity ligation following coincident detection of FLAG antibody and biotin antibody in neurons that had taken up azidohomoalanine (AHA); however, no newly synthesized FLAG protein was found in neurons expressing *cofilin* 5′UTR lacking the D1 region (Fig 3A). Furthermore, no newly synthesized FLAG protein was detected when neurons were treated with AHA and anisomycin, a translation inhibitor (Fig 3A). Together, our results indicate that cofilin is synthesized by IRES-mediated translation in neurons.

We next examined whether cofilin expression prefers IRES-mediated translation to canonical cap-dependent translation in neurons. mTOR phosphorylates 4E-BP1, a repressor of mRNA translation, which makes 4E-BP1 dissociate from cap-binding complex and subsequently allows mRNA translation (Choo *et al*, 2008). Thus, RAD001, an inhibitor of mTOR, negatively affects canonical cap-dependent translation. To examine whether mTOR signaling pathways affect cofilin expression, we treated Neuro2A cells with RAD001 for up to 9 h (Fig 3B). We found no reduction in the level of cofilin expression, while phosphorylation sites of ribosomal protein S6, a downstream target of mTOR signaling, were decreased during the treatment. We also used cycloheximide (CHX) that blocks translation elongation regardless of cap-dependent or cap-independent translation. CHX treatment profoundly reduced cofilin expression, but did not significantly alter the levels of phospho-rpS6, suggesting that cofilin is less stable compared to ribosomal protein S6. Hence, when elongation is blocked, the level of cofilin decreases. These results also imply that cofilin expression is not a downstream target of mTOR pathways. Next, to further verify that expression of cofilin in neurons depends on cap-independent mechanism, we reduced eIF4E, eukaryotic initiation factor-4E, by using *eIF4E* siRNA. The level of eIF4E was decreased, and subsequently, the c-Myc expression was also reduced (Fig 3C). In contrast, the cofilin protein expression showed increase (Fig 3C). Note that the cofilin level was slightly increased 9 h after RAD001 treatment (Fig 3B). It is plausible that blocking cap-dependent translation by reduction of eIF4E may enhance IRES-mediated *cofilin* translation by allowing more resource for IRES-mediated protein synthesis. Note that GAPDH has a long half-life (Franch *et al*, 2001), so no change was detected during the experimental condition. In addition, we found that the IRES activity of *cofilin* 5′UTR measured using bicistronic reporter system is significantly higher in neuronal cell lines compared to that of non-neuronal cell lines (Appendix Fig S3). Previously, *Apaf-1* IRES activity was also reported to be higher in neuronal cell lines (Mitchell *et al*, 2003). Altogether, our data imply that *cofilin* mRNA translation indeed prefers IRES-mediated mechanism to canonical cap-dependent translation in neurons.

Cofilin overexpression enhances axonal growth cone extension through IRES-mediated translation

Having demonstrated that IRES-mediated translation can regulate cofilin expression in neurons, we next examined whether endogenous cofilin expression is indeed regulated by IRES-mediated translation. Using the CRISPR–Cas9 system, we generated a genome-edited Neuro2A cell line lacking the D1 region of *cofilin* 5′UTR (Fig 4A), which enabled us to examine whether endogenous *cofilin* mRNA is indeed translated by IRES-mediated mechanism. We first identified a cell line that specifically deleted the D1 region of *cofilin* 5′UTR in the genome (Fig 4B). In this genome-edited cell

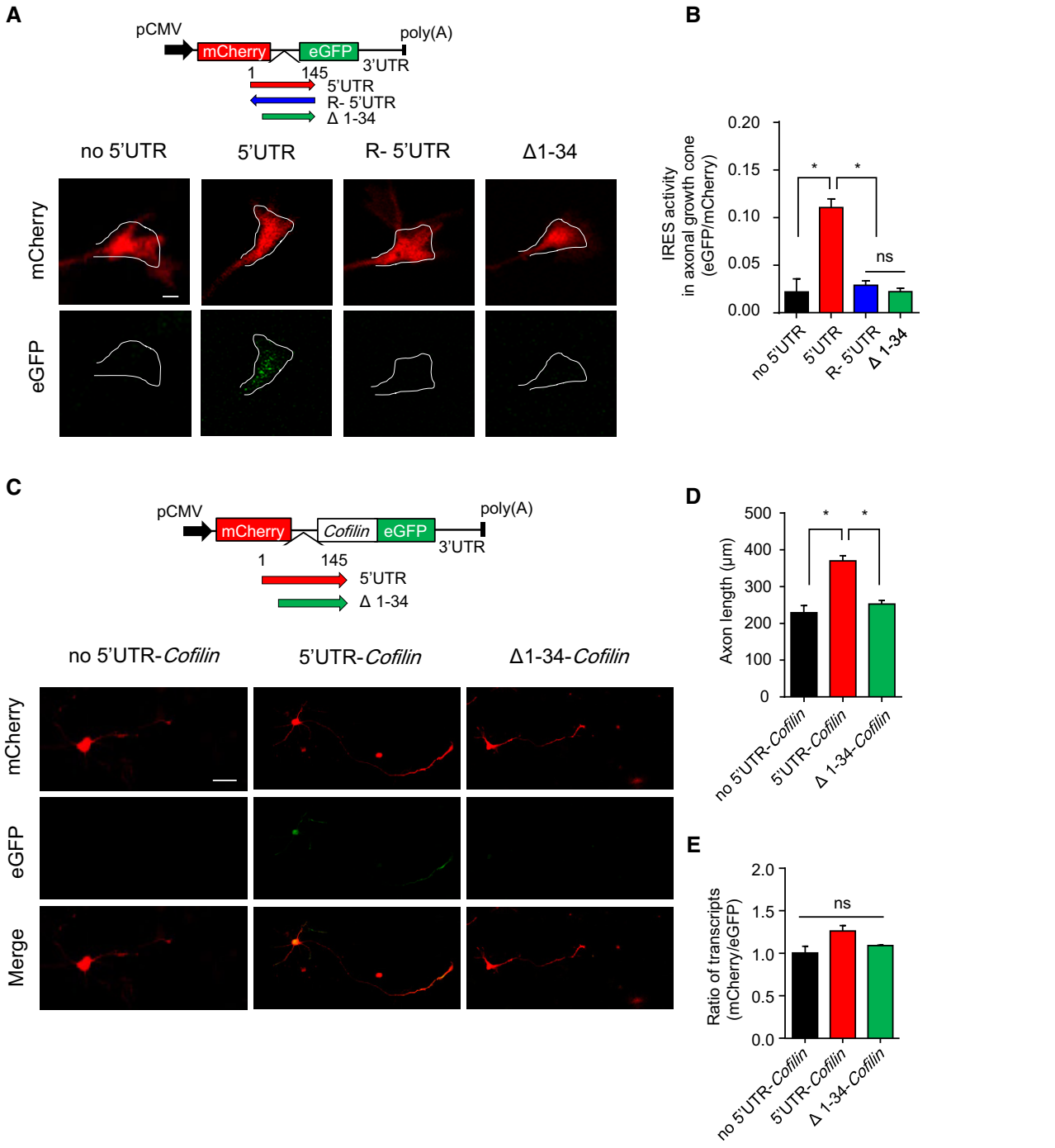

Figure 2. IRES-mediated *cofilin* translation extends axon growth.

A A bicistronic reporter system using mCherry and eGFP fluorescent reporters was adopted to determine IRES activity in hippocampal primary neurons. 5′UTR of *cofilin*, reversely oriented 5′UTR (R-5′UTR), or 5′UTR with Δ1–34 (Δ1–34) was inserted to the intercistronic region of the bicistronic reporter vector, respectively. These vectors were transfected to neurons at DIV1 (days *in vitro*) and IRES activity measured at DIV3. Growth cones were outline by white line. Scale bar = 2 μm.

B IRES activity was determined by the ratio of mCherry/eGFP signals in axonal growth cones at DIV3. *$P < 0.0001$, $N = 15$ neurons. Values shown are mean ± SEM and are tested for statistical significance by one-way ANOVA followed by Bonferroni *post hoc* test.

C Cofilin was expressed in hippocampal primary neurons by IRES-mediated translation. 5′UTR-*cofilin-eGFP* or 5′UTR(ΔD1)-*cofilin-eGFP* construct was inserted into the intercistronic region. The vectors were transfected at DIV1, and the axon length of neurons was measured at DIV3. Scale bar = 50 μm.

D IRES-mediated cofilin expression significantly increased axonal length compared to that of neurons lacking IRES-mediated cofilin translation. *$P < 0.0002$, $N = 42$ for neurons containing 5′UTR-*cofilin-eGFP*, and $n = 35$ for neurons having 5′UTR(ΔD1)-*cofilin-eGFP*. Values shown are mean ± SEM and are tested for statistical significance by one-way ANOVA followed by Bonferroni *post hoc* test.

E Real-time quantitative PCR for *mCherry* and *eGFP* mRNA transcripts was performed on vectors used in (B). $N = 3$ independent experiments. Values shown are mean ± SEM and are tested by one-way ANOVA followed by Bonferroni *post hoc* test.

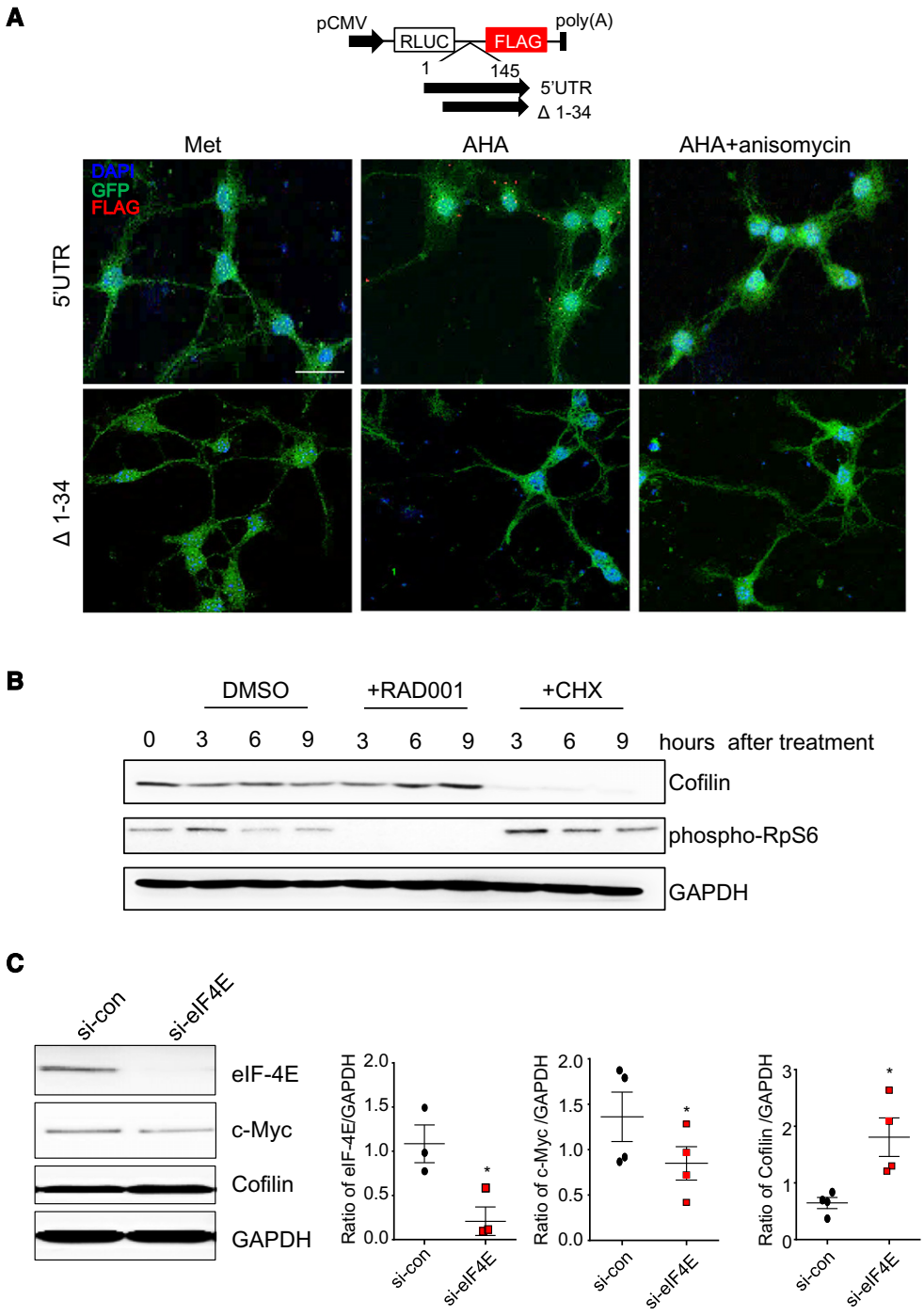

Figure 3. Cofilin synthesis in neurons utilizes IRES-mediated translation mechanism.

A Primary hippocampal neurons were transfected with a vector that expressed FLAG either under regulation of *cofilin* 5′UTR or *cofilin* 5′UTR with depleted D1 (Δ1–34) region at DIV 1. *eGFP* was co-transfected. FUNCAT-PLA was performed at DIV2 and azidohomoalanine (AHA) was treated for 2 h. AHA replaced methionine in neurons taking up AHA, which was labeled by biotin. The FUNCAT-PLA method using combination of biotin-labeled AHA and FLAG antibody was able to detect newly synthesized FLAG. Anisomycin blocked to synthesize new FLAG peptide in neurons containing *cofilin* 5′UTR-*FLAG*, and neurons containing *cofilin*-5′UTR (Δ1–34)-*FLAG* failed to express FLAG. Scale bar = 20 μm.

B Neuro2A cells treated with RAD001 showed little effect on cofilin expression, while cycloheximide (CHX) reduced *cofilin* translation. Conversely, a downstream target of mTOR, phospho-rpS6, showed no phosphorylation after 3 h of RAD001 treatment, while cycloheximide did not affect the level of phospho-rpS6.

C Expression of eIF4E and c-Myc was reduced by *eIF4E* siRNA transfection to Neuro2A cells, while cofilin level was increased. Cell lysates were prepared 3 days after transfection of siRNA. *$P < 0.05$, $N = 4$ independent experiments. Values shown are mean ± SEM and are tested by *t*-test.

Source data are available online for this figure.

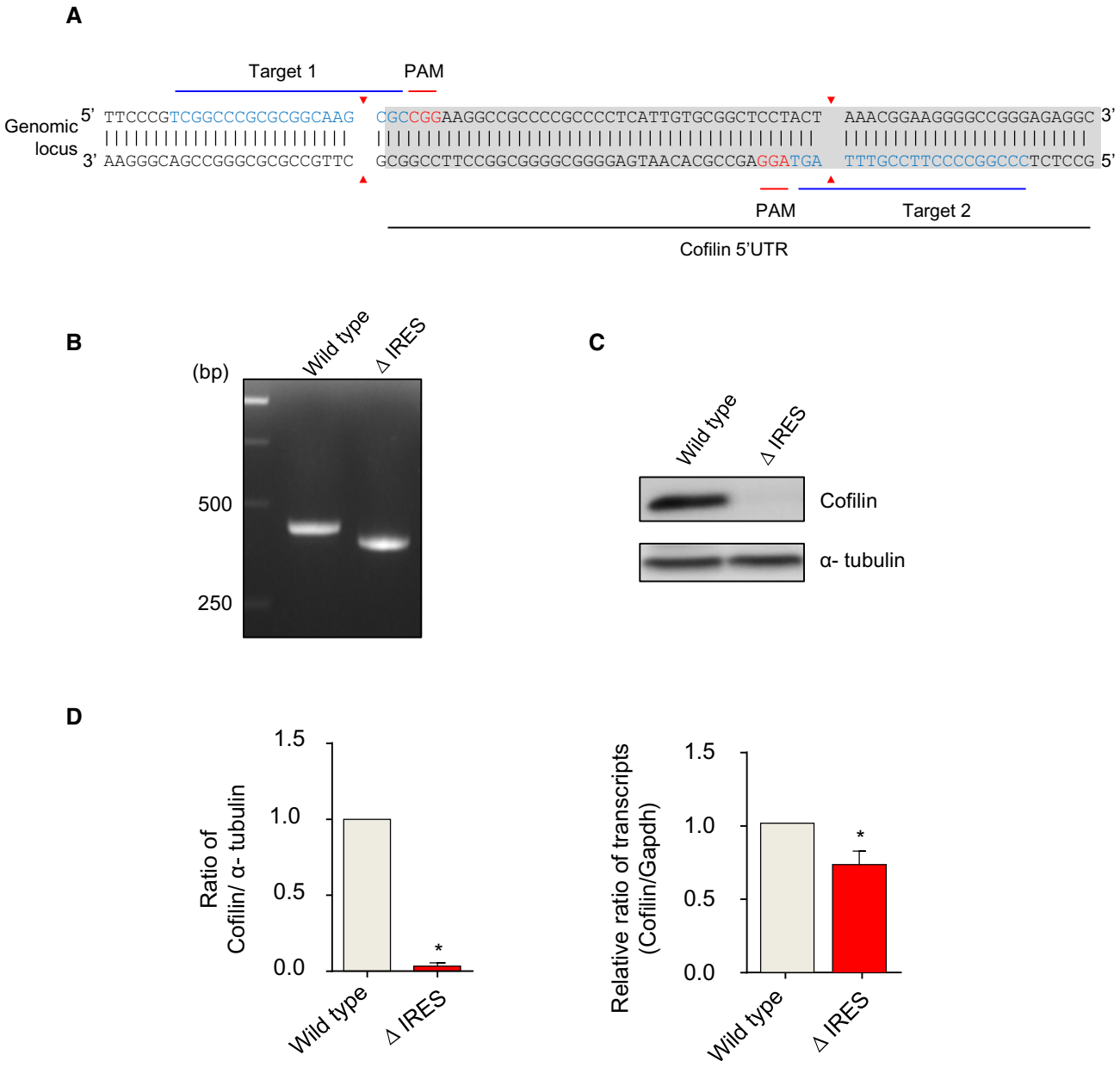

Figure 4. Cofilin expression prefers IRES-mediated translation to cap-dependent translation.

A, B The D1 region of *cofilin* 5′UTR was deleted using the CRISPR–Cas9 method; then, the genome-edited cell line was selected. Blue bars indicate the location of paired sgRNAs. Red arrowheads show expected deletion of the genomic DNA. Genotyping analysis identified a Neuro2A cell line lacking the D1 region.

C Cofilin protein expression was effectively reduced in the genome-edited cell line compared to the control.

D Left: Quantification of cofilin expression from (C). *$P < 0.0001$, $N = 3$ independent experiments. Right: Real-time quantitative PCR for *cofilin* mRNA transcripts in the genome-edited cell line showed a slight decrease. *$P < 0.04$, $N = 3$ independent experiments. Values shown are mean ± SEM and are tested by *t*-test.

Source data are available online for this figure.

line, the cofilin protein expression was completely missing (Fig 4C), although the amount of *cofilin* mRNA transcripts showed only a slight reduction in the genome-edited cells (Fig 4D). Together, our results suggest that cofilin expression in Neuro2A cells is indeed regulated by IRES-mediated translation.

Next, to further verify whether *cofilin* 5′UTR prefers IRES-mediated translation to cap-dependent mechanism, we designed a vector that has two different promoters to generate independent mRNA transcripts of *RLUC* and *LUC+* (modified firefly *luciferase* gene). RLUC translation in this vector can be achieved through both cap-dependent and IRES-mediated translation, or through only cap-dependent RLUC expression (Fig 5A). *LUC+* was translated by cap-dependent translation, and its activity was used as indicator of transfection efficiency. *Cofilin* 5′UTR, *cofilin* 5′UTR

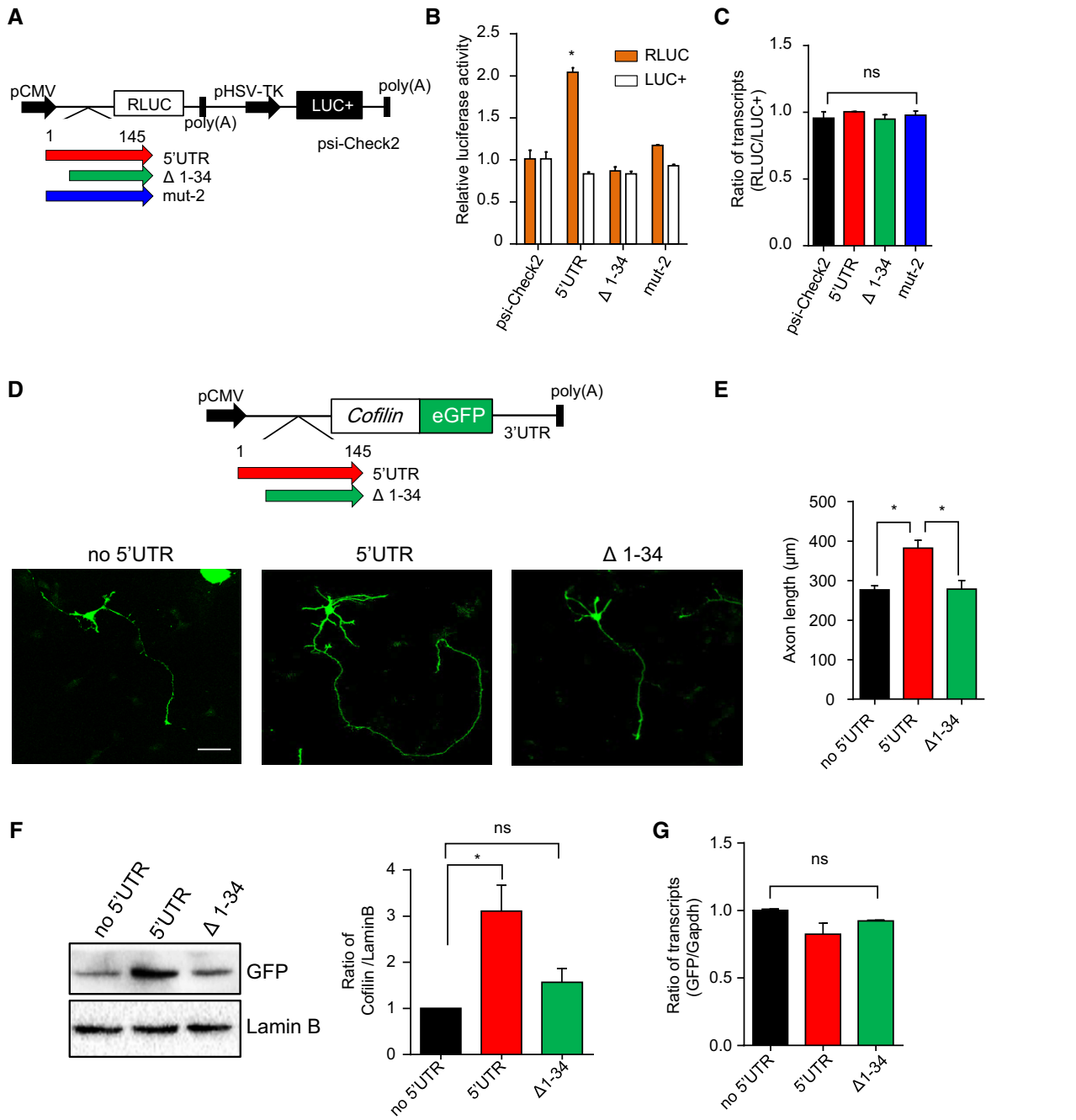

Figure 5. Overexpression of cofilin by IRES-mediated translation increases axonal growth cone extension.

A To verify the role of IRES activity in regulation of *cofilin* translation, *cofilin* 5′UTR, 5′UTR lacking D1 region, or 5′UTR having mutations in D1 was inserted to the upstream of *renilla luciferase* gene in psi-Check2 dual-reporter vector, which contains two promoters for *RLUC* and *LUC+* (modified firefly *luciferase* gene), respectively. The plasmids were transfected into Neuro2A cells, and dual-luciferase assays were performed.

B Insertion of 5′UTR increased RLUC, while no insert, 5′UTR lacking D1 region, or mutated 5′UTR did not increase RLUC activity. *$P < 0.0001$, $N = 4$. Values shown are mean ± SEM and are tested for statistical significance by one-way ANOVA followed by Bonferroni *post hoc* test.

C Real-time quantitative PCR for *RLUC* and *LUC+* mRNA transcripts showed no difference between cells transfected with the indicated constructs, $N = 3$. Values shown are mean ± SEM and tested for statistical significance by one-way ANOVA followed by Bonferroni *post hoc* test.

D, E Vectors containing 5′UTR-*cofilin*, 5′UTR-*cofilin* lacking IRES activity (Δ1–34), or no 5′UTR-*cofilin* were transfected to hippocampal primary neurons at DIV2, and axon length at DIV3 was measured. Axon length was significantly increased in neurons containing 5′UTR-*cofilin*, while neurons with 5′UTR-*cofilin* lacking IRES (Δ1–34) showed no axon extension compared to that of the control. *$P < 0.001$, $N = 30$ for each condition. Values shown are mean ± SEM and are tested for statistical significance by one-way ANOVA. Scale bar = 50 μm.

F, G GFP expression level in primary neurons containing the vector used above (D). *$P < 0.01$, $N = 3$. Values shown are mean ± SEM and are tested by one-way ANOVA followed by Bonferroni *post hoc* test.

Source data are available online for this figure.

lacking D1, or *cofilin* 5′UTR having mutations in D1 was inserted in front of the RLUC reporter. As expected, RLUC activity was significantly increased from the vector containing *cofilin* 5′UTR (Fig 5B). Interestingly, however, constructs without IRES activity (Δ1–34 or mut-2; Fig 1D) exhibited no difference in RLUC activity compared to that of vector without insert (Fig 5A), suggesting that the increase of RLUC expression in the vector allowing both cap-dependent and IRES-mediated expression of cofilin is mostly due to IRES-mediated translation. The ratio of *RLUC/LUC+* transcripts was not altered (Fig 5C). To further confirm the result, we prepared constructs with sequentially deleted nucleotides from the end of *cofilin* 5′UTR, which disrupts the D1 domain containing IRES activity (Appendix Fig S4A). RLUC expression was decreased according to the size of deletion in 5′UTR (Appendix Fig S4B), indicating that RLUC expression is mostly due to IRES activity resided in 5′UTR of *cofilin*. It is plausible, however, that the 5′UTR sequence may contain an element that suppresses cap-dependent translation. To examine the possibility, we also used the mut-2 construct (no IRES activity) with different deletions (Appendix Fig S4A and B). We reasoned that if an element hidden in 5′UTR of *cofilin* suppresses cap-dependent translation of RLUC, removing the element should increase the RLUC expression. Mut-2 construct with various deletions, however, did not increase RLUC expression (Appendix Fig S4B), suggesting that there is no element that suppresses cap-dependent translation, but cofilin expression preferentially utilizes IRES-mediated translation instead of cap-dependent translation. To further confirm the result in neurons, we transfected expression vectors to neurons, which allow translation of cofilin either by both cap-dependent and IRES-mediated mechanisms (5′UTR-*cofilin)* or by cap-dependent translation (5′UTR(Δ1–34)-*cofilin*) (Fig 5D–F). 5′UTR-*cofilin* expression significantly increased axon length, while 5′UTR-*cofilin* lacking IRES activity showed little effect on axonal growth cone extension, suggesting that extension of axonal growth cones is mostly due to IRES-mediated cofilin translation rather than cap-dependent cofilin expression. Note that no change was observed in neurons without *cofilin* 5′UTR (Fig 5E and F). Furthermore, deletion of IRES element of *cofilin* 5′UTR (5′UTR(Δ1–34)-*cofilin-eGFP)* did not interfere with normal cap-dependent translation of *eGFP*, since eGFP expression in neurons with 5′UTR (Δ1–34)-*cofilin-eGFP* is comparable to that of control that has no *cofilin* 5′UTR (Fig 5G).

IRES-mediated cofilin translation is required for axon outgrowth and turning

We demonstrated that deletion of IRES element in 5′UTR of *cofilin* by using CRISPR system abolished cofilin expression in the genome-edited cells. Furthermore, results in Fig 5 indicate that overexpression of cofilin regulates axonal growth cone extension through IRES-mediated translation; however, the endogenous roles of IRES-mediated *cofilin* translation in neurons are still not known. To this end, we designed vectors that could inhibit endogenous IRES activity by depleting IRES-transacting factors (ITAFs) required for IRES activity of *cofilin* 5′UTR. This was achieved by inserting 4 or 8 tandem repeats of *cofilin* 5′UTR-*eGFP* (Appendix Fig S5A), so that cells expressing these constructs could sequestrate ITAFs and consequently decrease endogenous IRES-mediated translation of *cofilin* in axonal growth cones. First, to test whether these constructs indeed reduce endogenous IRES activity of *cofilin* 5′UTR, we introduced 4 or 8 tandem repeats of *cofilin* 5′UTR-*eGFP* to Neuro2A cells together with the bicistronic reporter, where *cofilin* 5′UTR is inserted between *RLUC* and *FLUC*, to measure IRES activity (Appendix Fig S5A). Indeed, IRES activity of *cofilin* 5′UTR was decreased and correlated with the number of the tandem repeats (Appendix Fig S5B), while amounts of *RLUC* or *FLUC* mRNA transcripts were not altered (Appendix Fig S5C). Together, our results verify that the tandem repeats effectively reduced IRES activity. Next, to exclude the possibility that the tandem repeats may remove factors needed for canonical translation, we also examined whether expression of cap-dependent translation of *RLUC* in the bicistronic reporter system (pRF)—no insertion between *RLUC* and *FLUC*—is changed. Expression level of RLUC was not altered from the vector (Appendix Fig S5D), verifying that the multiple repeats of *cofilin* 5′UTR sequestered ITAFs required for only IRES activity, but had no effect on cap-dependent translation. Furthermore, we measured the level of cofilin and eGFP in Neuro2A cells transfected either with 8 tandem repeats of *cofilin* 5′UTR-*eGFP* or with 8 tandem repeats in the reverse orientation. Consistent with the reduction of IRES activity, we found that cofilin expression was significantly decreased in cells containing 8 tandem repeats of *cofilin* 5′UTR-*eGFP* compared to that of cells having reversely oriented 8 tandem repeats of *cofilin* 5′UTR-*eGFP* (Appendix Fig S5E). eGFP expression indicated that the vector containing 8 tandem repeats of *cofilin* 5′UTR-*eGFP* functioned normally in the cells. Conversely, no eGFP expression was detected in cells with reversely oriented 8 tandem repeats of *cofilin* 5′UTR-*eGFP* (Appendix Fig S5E). To further verify that tandem repeats do not change the general translation in the cells, we used the FUNCAT method. Instead of detecting a specific newly synthesized protein, we adopt this method to find general protein synthesis by detecting AHA that replaced methionine in any proteins. AHA was labeled with biotin, which was then detected by anti-biotin antibody. As expected, biotin level of cells having 8 tandem repeats of *cofilin* 5′UTR-*eGFP* was indistinguishable to that of cells containing reversely oriented 8 tandem repeats of *cofilin* 5′UTR-*eGFP* (Appendix Fig S5F and G). Cells were also cultured together with AHA and anisomycin, which showed a significant decrease in the biotin level in cells containing either 8 tandem repeats or reversely oriented 8 tandem repeats of *cofilin* 5′UTR-*eGFP*. Our results further support that 8 tandem repeats of *cofilin* 5′UTR-*eGFP* allows depletion of ITAF for IRES-mediated translation, leading to reduced IRES activity but normal canonical translation mechanism. It is important to note that NIH 3T3 cells containing tandem repeats of *cofilin* 5′UTR-*eGFP* did not express eGFP, and cofilin expression was not different between NIH 3T3 cell lines containing 8 tandem repeats and reversely oriented 8 tandem repeats of *cofilin* 5′UTR-*eGFP* (Appendix Fig S6A and B). This result suggests that ITAFs required for *cofilin* 5′UTR IRES activity are not available in NIH 3T3 cell line, which is consistent with the result showing low cofilin IRES activity measured using bicistronic reporter system in the same cell lines (Appendix Fig S3). Together, our data imply that cofilin expression is regulated by IRES-mediated translation in neurons.

Next, to further examine the physiological role of IRES-mediated cofilin translation in axonal growth cones, we then transfected the construct containing 8 tandem *cofilin* 5′UTR-*eGFP* to primary hippocampal neurons. Cofilin expression in axonal growth cones as well as in the cell body was significantly decreased compared to

those of the control (Appendix Figs S6C, and S7A and B). We next investigated the consequences of decreased endogenous IRES-mediated *cofilin* translation in axonal growth cones and found that neurons containing 8 tandem repeats of *cofilin* 5′UTR-*eGFP* generated significantly shorter axon length compared to that of neurons with reversely oriented 8 tandem repeats (Appendix Fig S7C and D). This result suggests that IRES-mediated *cofilin* translation is required for axon extension. Since cofilin also plays a key role in axonal growth cone steering responding to a repellent such as Sema3A (Aizawa *et al*, 2001), we then asked whether reduction of IRES-mediated *cofilin* translation changes the response of axonal growth cones to Sema3A. To this end, we measured turning angles of individual axonal growth cones containing 8 tandem repeats of *cofilin* 5′UTR-*eGFP* or with 8 reversely oriented tandem repeats in the Dunn chamber (Yam *et al*, 2009; Wang *et al*, 2016) with or without Sema3A gradient (Appendix Fig S7E and F). Growth cones from the control neurons steered away from Sema3A gradient; however, neurons containing 8 tandem repeats of *cofilin* 5′UTR-*eGFP* did not (Appendix Fig S7E and F). Together, these results indicate that IRES-mediated *cofilin* translation is required for both axon outgrowth and growth cone steering.

Since a previous report showed that the *cofilin* 5′UTR contains polypyrimidine tract binding protein (PTB)-dependent IRES motif (Mitchell *et al*, 2005) and neuronal PTB (nPTB) stimulated *Apaf-1* IRES activity (Mitchell *et al*, 2003), we tested whether nPTB acts as ITAF for *cofilin* IRES activity. We first examined whether nPTB binds to *cofilin* mRNA transcripts. Figure 6A demonstrates that nPTB indeed associated with the *cofilin* transcripts. Reducing nPTB using *nPTB* siRNA decreased *cofilin* IRES activity (Fig 6B) and cofilin protein level in neurons, while amounts of *cofilin* mRNA transcripts were not altered (Fig 6C–E). Importantly, *nPTB* siRNA also efficiently reduced the neuronal axon length (Fig 6F and G) and significantly impaired response to Sema3A treatment in the Dunn chamber assay (Fig 6H and I). Together, our data strongly suggest that nPTB is ITAF for IRES-mediated *cofilin* translation in neuron.

Discussion

Here, we show that IRES-mediated translation is critical in normal physiological environments. We found that (i) *cofilin* 5′UTR harbors IRES-mediated translation; (ii) IRES-mediated cofilin expression extends axonal growth; (iii) decreasing IRES-mediated cofilin translation in axonal growth cones inhibits axonal outgrowth as well as repressing axonal growth cone steering due to Sema3A; (iv) *cofilin* 5′UTR prefers IRES-mediated translation to cap-dependent translation; (v) nPTB plays as ITAF for IRES-mediated *cofilin* translation; and (vi) *cofilin* 5′UTR is highly conserved among mammalians.

It is interesting to note that nucleotide sequences of *cofilin* 5′UTR are highly conserved among human, monkey, whale, dog, and mouse (Appendix Fig S8), however no homology is found in *Xenopus*, zebrafish, fly, or yeast. While the sequence of cofilin protein and its role on cytoskeleton dynamics are conserved from yeast to mammals, the nucleotide sequence of *cofilin* 5′UTR is preserved only in mammals. This finding suggests that IRES-mediated cofilin translation in neurons seems to be a highly elaborate mechanism that contributes to sophisticated mammalian brain development.

It is also suggested that semaphorins induce cofilin translation via eIF2α in *Caenorhabditis elegans* (Chisholm, 2008). Phospho-eIF2α represses general translation, but can also activate translation of specific messages containing uORFs, such as GCN4 in the yeast amino acid starvation response. Hence, we tested whether eIF2α may affect translation of cofilin (via eIF2α) and not the IRES elements. To address this, we depleted eIF2α using *eIF2α* siRNA (Appendix Fig S9). We found that cofilin translation was not affected, suggesting that cofilin translation is IRES-mediated, not by eIF2α. We also identified nPTB as the ITAF for cofilin IRES activity.

Our work reveals a physiological role for IRES-mediated cofilin translation in controlling axon growth and axonal growth cone navigation, which are critical processes for proper wiring of the complex neuronal networks in the brain during development. We believe that IRES-mediated translation mechanism will play key roles in regulating protein synthesis in diverse physiological conditions.

Figure 6. nPTB is required for IRES-mediated *cofilin* translation.

A Neuro2A cell extracts were used to test whether nPTB is binding to the biotinylated *cofilin* 5′UTR. Streptavidin–biotin RNA affinity purification was performed, and purified samples were separated by SDS–PAGE and immunoblotted with antibody against nPTB. For competition assay, nonlabeled *cofilin* 5′UTR (10×) was also co-incubated.

B IRES activity was determined with a bicistronic reporter system used in Fig 1A together with control siRNA or *nPTB* siRNA in Neuro2A cells. $*P < 0.001$, $N = 3$. Values shown are mean ± SEM and are tested for statistical significance by two-way ANOVA followed by Bonferroni *post hoc* test.

C Cofilin expression level was decreased in Neuro2A cells containing *nPTB* siRNA compared to that of control siRNA. GAPDH was a loading control. Amounts of *cofilin* mRNA transcripts were not altered. $N = 3$. Values shown are mean ± SEM, and tested for statistical significance by one-way ANOVA followed by *t*-test.

D, E Cofilin expression was reduced in primary hippocampal neurons containing *nPTB* siRNA compared to that of neurons having control siRNA. *nPTB* siRNAs and *GFP* vector were co-transfected to neurons at DIV1 and analyzed at DIV3. Immunocytochemistry was performed using antibodies against cofilin and nPTB, respectively. Scale bar = 20 μm. $*P < 0.05$, $**P < 0.01$, $N = 18$ for each condition. Values shown are mean ± SEM and are tested for statistical significance by *t*-test.

F, G Axon length was significantly decreased in neurons containing *nPTB* siRNA. Experimental condition was the same as in (D). Scale bar = 50 μm. $*P < 0.001$, $N = 28$ for each condition. Values shown are mean ± SEM and are tested for statistical significance by *t*-test.

H The Dunn chamber experiments produced trajectory plots on axonal growth cone turning response to Sema3A gradient. Axons containing *nPTB* siRNA did not turn away from Sema3A gradient, while axons having control siRNA repelled from Sema3A. Sema3A gradient was established to increase along the *y*-axis, and all axons are re-positioned to it accordingly for clarity. Black lines show the initial 10 μm of axons, and different colors represent the initial turning angles of axonal growth cones over a 2-h recording period. To reduce complexity of the figure, only 10 representative traces are shown. $N > 12$ transfected neurons were analyzed for each group.

I Axonal growth cones of neurons containing *nPTB* siRNA did not show any response in the Dunn chamber assay regardless of the presence of Sema3A gradient, while axonal growth cones with control siRNA were notably turned away from Sema3A gradient. $*P < 0.001$. Values shown are mean ± SEM and are tested for statistical significance by two-way ANOVA followed by Bonferroni *post hoc* test.

Source data are available online for this figure.

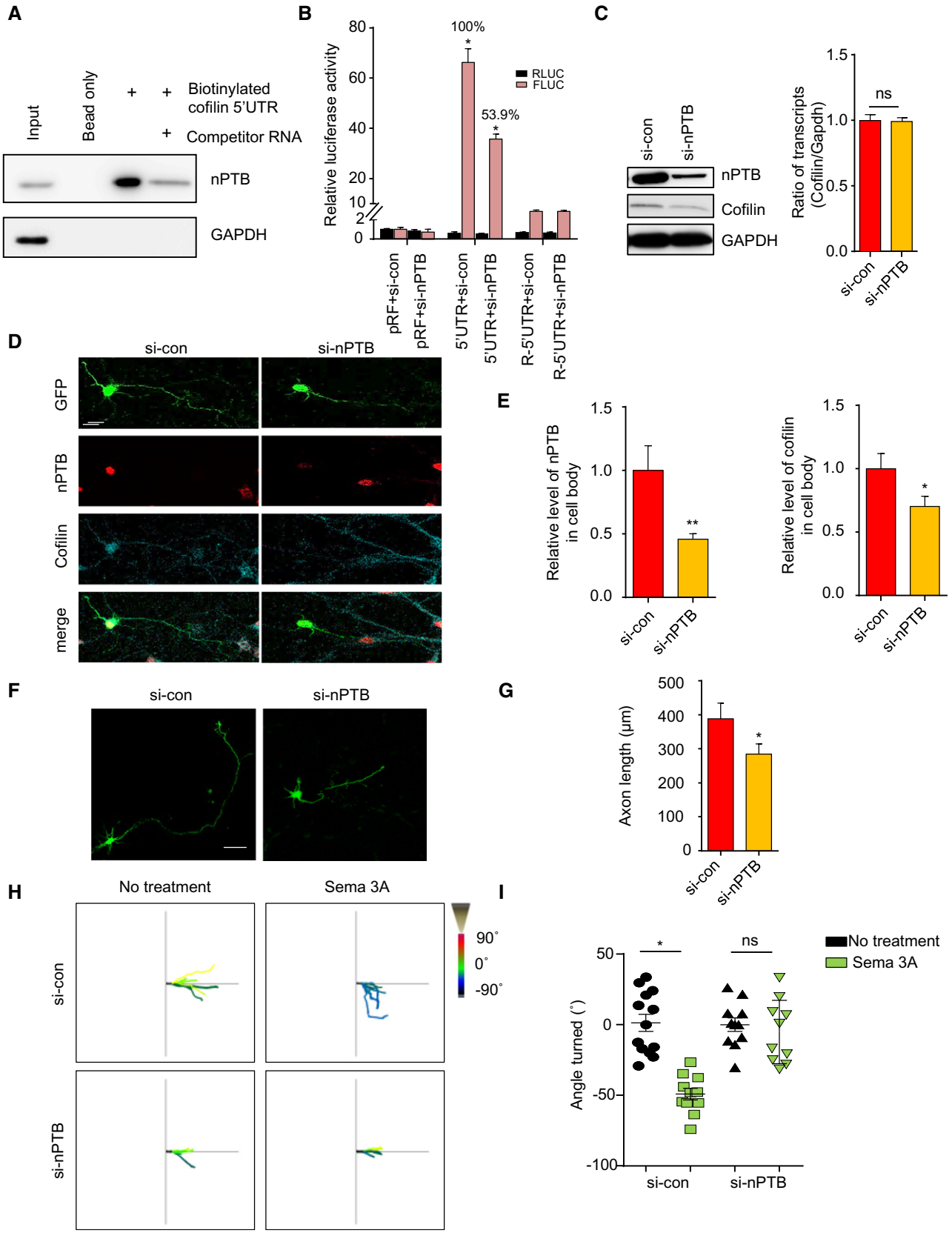
A
Input
Bead only
+ + Biotinylated cofilin 5'UTR
+ Competitor RNA
nPTB
GAPDH
B
Relative luciferase activity
RLUC
FLUC
100%
53.9%
pRF+si-con
pRF+si-nPTB
5'UTR+si-con
5'UTR+si-nPTB
R-5'UTR+si-con
R-5'UTR+si-nPTB
C
si-con
si-nPTB
nPTB
Cofilin
GAPDH
Ratio of transcripts (Cofilin/Gapdh)
ns
D
si-con
si-nPTB
GFP
nPTB
Cofilin
merge
E
Relative level of nPTB in cell body
Relative level of cofilin in cell body
F
si-con
si-nPTB
G
Axon length (μm)
H
No treatment
Sema 3A
si-con
si-nPTB
90˚
0˚
-90˚
I
Angle turned (˚)
ns
No treatment
Sema 3A

Figure 6.

Materials and Methods

Animals

Animals were used in accordance with protocols approved by the Animal Care and Use Committees of the Ulsan National Institute of Science and Technology. C57BL/6 mouse strain was purchased from Hyochang Science.

Cell culture

Hippocampal cultures were prepared from E18 mouse embryos as described previously (Wang *et al*, 2012). Briefly, 24-well plate containing 12-mm glass coverslips or 35-mm glass-bottom dishes (WillCo Wells) coated with poly-D-lysine (50 μg/ml; Sigma) was used to seed neurons. Lipofectamine™ 2000 (Invitrogen) was used to transfect neurons with different DNA vectors at DIV1. Neuro2A cells were cultured in Dulbecco's modified Eagle's medium (Gibco) with 10% fetal bovine serum (Gibco) and 1% penicillin–streptomycin.

Plasmid construction

The 5′UTR of mouse *cofilin* was cloned by PCR from its cDNA (NM_007689.5) using primers (forward: ACGCGTCGACGCCGGAA GGCCGCCCCG; reverse: TCCCCCCGGGGTTTCCGGAAACGAAAGG GAGAC), which then was inserted into the pRF bicistronic vector that contains both renilla luciferase (RLUC) and firefly luciferase (FLUC). Various deleted and reversely oriented 5′UTR constructs were prepared from the 5′UTR of *cofilin*. mCherry and eGFP fluorescent proteins attached with myristoylation signal replaced RLUC and FLUC for IRES activity in axonal growth cones. Four or eight tandem repeats of *cofilin* 5′UTR-*eGFP* was inserted to pEGFP-C1 vector.

mRNA transfection

A bicistronic vector was first linearized; then, the reporter mRNAs were synthesized by *in vitro* transcription with SP6 polymerase (Roche) in the presence of the cap analog $m^7G(5')ppp(5')$ (Roche). The capped bicistronic mRNA reporters were transiently transfected into Neuro2A cells using Lipofectamine™ 2000 (Invitrogen) and incubated for 12 h.

Luciferase assay

Cells were harvested and re-suspended in luciferase lysis buffer (Promega), followed by incubation on ice for 10 min. Cell debris was removed by centrifugation at 20,000 *g* at 4°C for 10 min, and the supernatants were used for the luciferase assay. Firefly and renilla luciferase activities were determined using the Dual-Luciferase Reporter Assay System (Promega) according to the manufacturer's instructions. The ratio of firefly luciferase to renilla luciferase activity was defined as IRES activity.

β-Galactosidase assay

Cells transfected with a β-galactosidase expression vector were harvested and re-suspended in luciferase lysis buffer (Promega), followed by incubation on ice for 10 min. Cell lysates were incubated with the reagents [PBS containing 5 mM EDTA, chlorophenol red-β-D-galactopyranoside (CPRG), β-gal buffer] at room temperature. After confirming end point, β-galactosidase activities were measured using a plate reader at a wavelength of 570 nm.

Quantitative real-time reverse transcription PCR

Quantitative real-time RT–PCR was performed as described previously (Kim *et al*, 2015). Briefly, TRI reagent (Molecular Research Center) was used to isolate total RNAs, followed by reverse transcription using ImProm-II™ Reverse Transcription System (Promega). Next, quantitative real-time PCR (Applied Biosystems) with the SYBR Green Master Mix (Roche) was used to analyze the expression level of mRNA transcripts.

Live imaging

Hippocampal neurons were transfected with 5′UTR-*cofilin* or 5′UTR (lacking IRES activity)-*cofilin* to investigate axonal growth cone extension. Live imaging was performed in an environmental chamber maintaining 37°C and 5% CO_2. Image intervals were 30 s for 1 h (total 120 frames) using Zeiss LSM 780 confocal microscope with 40× water objective (Nikon Plan Apo, NA 1.3). The rate of axon growth was analyzed by ImageJ.

Immunocytochemistry

Hippocampal primary neurons were fixed in pre-warmed 4% paraformaldehyde for 15 min at room temperature (RT) and then washed twice with PBS for 10 min. Next, neurons were permeabilized by PBS containing 0.5% Triton X-100 for 15 min at RT and blocked for 1 h at RT with PBS containing 1% BSA. Immunostaining was performed by cofilin antibody (Abcam; 1:100) at 4°C overnight, followed by addition of Alexa-conjugated secondary antibody (Invitrogen 1:2,000) for 1 h at RT. Images were taken with LSM 780 confocal microscope (Zeiss).

CRISPR–Cas9 method

To generate the sgRNA expression construct, we used pSpCas9(BB)-2A-Puro (PX459) plasmid obtained from Addgene (Addgene #62988). Target sgRNAs were designed and prepared as described previously (Ran *et al*, 2013), and off-target effects of sgRNA candidates were checked using the online CRISPR Design tool (http://crispr.mit.edu). Target dsDNAs were generated by annealing two oligonucleotides: target 1 (top: TCGGCCCGCGCGGCAAGCGC; bottom: GCGCTTGCCGCGCGGGCCGA) and target 2 (top: ACTAAA CGGAAGGGGCCGGG; bottom: CCCGGCCCCTTCCGTTTAGT). Then, target dsDNAs were cloned into the px459 vectors. Genomic DNA sequencing was performed with primers (forward: CCTCTGGCTC AGAGCGTTTT; reverse: TGGGATACCAAGACCGCTTC) to verify genomic deletion.

Western blotting

Immunoblot analysis was performed with polyclonal anti-cofilin (Abcam 42824, 1:1,000), monoclonal anti-phospho-rpS6 (Cell

signaling #9206, 1:1,000), monoclonal anti-GFP (Santa Cruz 9996, 1:2,000), monoclonal anti-eIF4E (Abcam 171091, 1:500), monoclonal anti-c-Myc (Santa Cruz 40, 1:1,000), and monoclonal anti-α-tubulin (Santa Cruz 5286 1:1,000) as primary antibodies. HRP-conjugated secondary antibodies were visualized by ECL solution and a LAS-4000 chemiluminescence detection system.

Fluorescent noncanonical amino acid tagging–proximity ligation assay (FUNCAT-PLA)

FUNCAT-PLA was performed as described (tom Dieck *et al*, 2015). Plasmids were transfected into mouse hippocampal primary neurons at DIV1. For metabolic labeling, neurons at DIV2 were cultured in Met-free DMEM (Gibco, Cat. 21013-024) for 30 min, and then, 4 mM L-azidohomoalanine (AHA, Invitrogen, Cat. C10102) was added for 2 h. As a negative control, 4 mM methionine (Sigma, M0960000) instead of AHA was used. Neurons were fixed with 4% PFA–sucrose for 20 min and permeabilized with 0.5% Triton X-100. After blocking with 4% goat serum (Gibco, Cat. PCN5000), click reaction was performed by adding chemicals: 200 mM TBTA (Sigma, Cat. 678937), 500 mM TCEP (Sigma, Cat. 646547), 25 mM biotin-alkyne (Jena Bioscience, Cat. CLK-TA105-25), and 200 mM $CuSO_4$ (Sigma, Cat. C1297). Then, proximity ligation assay (PLA) using Duolink reagents (Sigma, Cat. DUO92101) was performed according to the manufacturer's recommendations. For primary antibodies, we used biotin antibody (1:1,500, Sigma, Cat. B7653) and Flag antibody (1:1,500, Sigma, Cat. F7425). For metabolic labeling in Neuro2A cells, AHA-labeled proteins were stained with biotin antibody (1:1,000) at 4°C overnight after click reaction, followed by addition of Alexa-conjugated secondary antibody (Invitrogen, 1:2,500).

Axonal growth cone steering assay using the Dunn chamber

Mouse hippocampal neurons were plated on 22-mm square coverslips (Fisher Scientific), and transfected at DIV1. Sema3A (R&D Systems) gradient was established by adding it to the outer well of the Dunn chamber. The Dunn chamber assay was performed at DIV3. Images were taken every 5 min for 2 h by using Zeiss LSM 780 confocal microscope with a 20× objective (Nikon Plan Apo, NA 0.8). The Dunn chamber axon guidance assays and analyses were performed as reported previously (Yam *et al*, 2009; Wang *et al*, 2016).

Streptavidin–biotin RNA affinity purification assay

Cofilin 5′UTR was synthesized by *in vitro* transcription with T7 RNA polymerase (Roche) in the presence of biotinylated UTP. Biotin-labeled *cofilin* 5′UTR was then incubated with cytoplasmic extracts from Neuro2A cells in dialysis buffer [10 mM HEPES, 90 mM KOAC, 1.5 mM MgOAc, 2.5 mM DTT]. In competition experiments, 10× unlabeled *cofilin* 5′UTR was also added to the reaction buffer containing biotin-labeled *cofilin* 5′UTR. After 30-min incubation, samples were pre-cleared with streptavidin agarose resin (Thermo Scientific #20349) at 4°C overnight in a rotary mixer. After washing three times with dialysis buffer (+ 1% NP-40), resin-bound proteins were eluted and used for immunoblotting.

Multiple sequence alignments

Multiple sequence alignment was generated by ClustalX, followed by preparation of a guide tree of the sequences according to the pairwise similarity of the sequences.

Statistical analysis

Statistical significance was measured by Student's *t*-test, one-way ANOVA, or two-way ANOVA followed by Bonferroni *post hoc* test using GraphPad Prism 5.0 software (GraphPad Software).

Expanded View for this article is available online.

Acknowledgements
This work was supported by the Leading Research Program, National Research Foundation of Korea (NRF) grant funded by the Korean government (MEST) (2016R1A3B1905982) to K-T. Min; and by BK21 Plus (10Z20130012243) funded by the Ministry of Education, Science and Technology, the Brain Research Program through the National Research Foundation of Korea (NRF) (2017023478), KBRI Basic Research Program through Korea Brain Research Institute (KBRI) (17-BR-01) funded by the Ministry of Science, ICT and Future Planning, and the Cooperative Research Program for Agriculture Science and Technology Development (PJ01121602) of the Rural Development Administration, Korea, to K-T. Kim.

Author contributions
J-HC designed and performed most experiments; WW conducted the Dunn chamber assay; DP contributed to CRISPR experiment; S-HK provided intellectual input for performing tandem repeat experiment; K-TK supervised the project; K-TM conceived and supervised the study, and wrote the manuscript with contribution from J-HC.

Conflict of interest
The authors declare that they have no conflict of interest.

References

Aizawa H, Wakatsuki S, Ishii A, Moriyama K, Sasaki Y, Ohashi K, Sekine-Aizawa Y, Sehara-Fujisawa A, Mizuno K, Goshima Y, Yahara I (2001) Phosphorylation of cofilin by LIM-kinase is necessary for semaphorin 3A-induced growth cone collapse. *Nat Neurosci* 4: 367 – 373

Arber S, Barbayannis FA, Hanser H, Schneider C, Stanyon CA, Bernard O, Caroni P (1998) Regulation of actin dynamics through phosphorylation of cofilin by LIM-kinase. *Nature* 393: 805 – 809

Audigier S, Guiramand J, Prado-Lourenco L, Conte C, Gonzalez-Herrera IG, Cohen-Solal C, Récasens M, Prats A-C (2008) Potent activation of FGF-2 IRES-dependent mechanism of translation during brain development. *RNA* 14: 1852 – 1864

Bamburg JR, Bernstein BW (2010) Roles of ADF/cofilin in actin polymerization and beyond. *F1000 Biol Rep* 2: 62

Bellon A, Iyer A, Bridi S, Lee FC, Ovando-Vazquez C, Corradi E, Longhi S, Roccuzzo M, Strohbuecker S, Naik S, Sarkies P, Miska E, Abreu-Goodger C, Holt CE, Baudet ML (2017) miR-182 regulates Slit2-mediated axon guidance by modulating the local translation of a specific mRNA. *Cell Rep* 18: 1171 – 1186

Buck KB, Zheng JQ (2002) Growth cone turning induced by direct local modification of microtubule dynamics. *J Neurosci* 22: 9358 – 9367

Chen TJ, Gehler S, Shaw AE, Bamburg JR, Letourneau PC (2006) Cdc42 participates in the regulation of ADF/cofilin and retinal growth cone filopodia by brain derived neurotrophic factor. *J Neurobiol* 66: 103 – 114

Chisholm AD (2008) Semaphorin signaling in morphogenesis: found in translation. *Genes Dev* 22: 955 – 959

Choo AY, Yoon SO, Kim SG, Roux PP, Blenis J (2008) Rapamycin differentially inhibits S6Ks and 4E-BP1 to mediate cell-type-specific repression of mRNA translation. *Proc Natl Acad Sci USA* 105: 17414 – 17419

Colussi TM, Costantino DA, Zhu J, Donohue JP, Korostelev AA, Jaafar ZA, Plank TD, Noller HF, Kieft JS (2015) Initiation of translation in bacteria by a structured eukaryotic IRES RNA. *Nature* 519: 110 – 113

Dent EW, Callaway JL, Szebenyi G, Baas PW, Kalil K (1999) Reorganization and movement of microtubules in axonal growth cones and developing interstitial branches. *J Neurosci* 19: 8894 – 8908

Dent EW, Gupton SL, Gertler FB (2011) The growth cone cytoskeleton in axon outgrowth and guidance. *Cold Spring Harb Perspect Biol* 3: a001800

tom Dieck S, Kochen L, Hanus C, Heumuller M, Bartnik I, Nassim-Assir B, Merk K, Mosler T, Garg S, Bunse S, Tirrell DA, Schuman EM (2015) Direct visualization of newly synthesized target proteins *in situ*. *Nat Methods* 12: 411 – 414

Fernandez J, Yaman I, Merrick WC, Koromilas A, Wek RC, Sood R, Hensold J, Hatzoglou M (2002) Regulation of internal ribosome entry site-mediated translation by eukaryotic initiation factor-2α phosphorylation and translation of a small upstream open reading frame. *J Biol Chem* 277: 2050 – 2058

Filbin ME, Kieft JS (2009) Toward a structural understanding of IRES RNA function. *Curr Opin Struct Biol* 19: 267 – 276

Franch HA, Sooparb S, Du J, Brown NS (2001) A mechanism regulating proteolysis of specific proteins during renal tubular cell growth. *J Biol Chem* 276: 19126 – 19131

Gehler S, Shaw AE, Sarmiere PD, Bamburg JR, Letourneau PC (2004) Brain-derived neurotrophic factor regulation of retinal growth cone filopodial dynamics is mediated through actin depolymerizing factor/cofilin. *J Neurosci* 24: 10741 – 10749

Graber TE, Holcik M (2007) Cap-independent regulation of gene expression in apoptosis. *Mol BioSyst* 3: 825 – 834

Grintsevich EE, Yesilyurt HG, Rich SK, Hung RJ, Terman JR, Reisler E (2016) F-actin dismantling through a redox-driven synergy between Mical and cofilin. *Nat Cell Biol* 18: 876 – 885

Gritsenko AA, Weingarten-Gabbay S, Elias-Kirma S, Nir R, de Ridder D, Segal E (2017) Sequence features of viral and human internal ribosome entry sites predictive of their activity. *PLoS Comput Biol* 13: e1005734

Hinnebusch AG, Ivanov IP, Sonenberg N (2016) Translational control by 5′-untranslated regions of eukaryotic mRNAs. *Science* 352: 1413 – 1416

Hsieh SH, Ferraro GB, Fournier AE (2006) Myelin-associated inhibitors regulate cofilin phosphorylation and neuronal inhibition through LIM kinase and Slingshot phosphatase. *J Neurosci* 26: 1006 – 1015

Kieft JS (2008) Viral IRES RNA structures and ribosome interactions. *Trends Biochem Sci* 33: 274 – 283

Kim TD, Woo KC, Cho S, Ha DC, Jang SK, Kim KT (2007) Rhythmic control of AANAT translation by hnRNP Q in circadian melatonin production. *Genes Dev* 21: 797 – 810

Kim DY, Kim W, Lee KH, Kim SH, Lee HR, Kim HJ, Jung Y, Choi JH, Kim KT (2013) hnRNP Q regulates translation of p53 in normal and stress conditions. *Cell Death Differ* 20: 226 – 234

Kim SH, Lee KH, Kim DY, Kwak E, Kim S, Kim KT (2015) Rhythmic control of mRNA stability modulates circadian amplitude of mouse Period3 mRNA. *J Neurochem* 132: 642 – 656

Lee P-T, Chao P-K, Ou L-C, Chuang J-Y, Lin Y-C, Chen S-C, Chang H-F, Law P-Y, Loh HH, Chao Y-S, Su T-P, Yeh S-H (2014) Morphine drives internal ribosome entry site-mediated hnRNP K translation in neurons through opioid receptor-dependent signaling. *Nucleic Acids Res* 42: 13012 – 13025

Liu QY (2015) Blocking IRES-mediated translation pathway as a new method to treat Alzheimer's disease. *J Med Hypotheses Ideas* 9: 57 – 60

Lowery LA, Van Vactor D (2009) The trip of the tip: understanding the growth cone machinery. *Nat Rev Mol Cell Biol* 10: 332 – 343

Martineau Y, Le Bec C, Monbrun L, Allo V, Chiu I-M, Danos O, Moine H, Prats H, Prats A-C (2004) Internal ribosome entry site structural motifs conserved among mammalian fibroblast growth factor 1 alternatively spliced mRNAs. *Mol Cell Biol* 24: 7622 – 7635

Martinez-Salas E (2008) The impact of RNA structure on picornavirus IRES activity. *Trends Microbiol* 16: 230 – 237

Mitchell SA, Spriggs KA, Coldwell MJ, Jackson RJ, Willis AE (2003) The Apaf-1 internal ribosome entry segment attains the correct structural conformation for function via interactions with PTB and unr. *Mol Cell* 11: 757 – 771

Mitchell SA, Spriggs KA, Bushell M, Evans JR, Stoneley M, Le Quesne JPC, Spriggs RV, Willis AE (2005) Identification of a motif that mediates polypyrimidine tract-binding protein-dependent internal ribosome entry. *Genes Dev* 19: 1556 – 1571

Olson CM, Donovan MR, Spellberg MJ, Marr MT II (2013) The insulin receptor cellular IRES confers resistance to eIF4A inhibition. *Elife* 2: e00542

Pelletier J, Sonenberg N (1988) Internal initiation of translation of eukaryotic mRNA directed by a sequence derived from poliovirus RNA. *Nature* 334: 320 – 325

Pfaendtner J, De La Cruz EM, Voth GA (2010) Actin filament remodeling by actin depolymerization factor/cofilin. *Proc Natl Acad Sci USA* 107: 7299 – 7304

Pinkstaff JK, Chappell SA, Mauro VP, Edelman GM, Krushel LA (2001) Internal initiation of translation of five dendritically localized neuronal mRNAs. *Proc Natl Acad Sci USA* 98: 2770 – 2775

Piper M, Anderson R, Dwivedy A, Weinl C, van Horck F, Leung KM, Cogill E, Holt C (2006) Signaling mechanisms underlying Slit2-induced collapse of Xenopus retinal growth cones. *Neuron* 49: 215 – 228

Ran FA, Hsu PD, Wright J, Agarwala V, Scott DA, Zhang F (2013) Genome engineering using the CRISPR-Cas9 system. *Nat Protoc* 8: 2281 – 2308

Ray PS, Das S (2002) La autoantigen is required for the internal ribosome entry site-mediated translation of Coxsackievirus B3 RNA. *Nucleic Acids Res* 30: 4500 – 4508

Schaefer AW, Schoonderwoert VT, Ji L, Mederios N, Danuser G, Forscher P (2008) Coordination of actin filament and microtubule dynamics during neurite outgrowth. *Dev Cell* 15: 146 – 162

Shi Y, Yang Y, Hoang B, Bardeleben C, Holmes B, Gera J, Lichtenstein A (2016) Therapeutic potential of targeting IRES-dependent c-myc translation in multiple myeloma cells during ER stress. *Oncogene* 35: 1015 – 1024

Srivastava T, Fortin DA, Nygaard S, Kaech S, Sonenberg N, Edelman AM, Soderling TR (2012) Regulation of neuronal mRNA translation by CaM-Kinase I phosphorylation of eIF4GII. *J Neurosci* 32: 5620 – 5630

Tilve S, Difato F, Chieregatti E (2015) Cofilin 1 activation prevents the defects in axon elongation and guidance induced by extracellular alpha-synuclein. *Sci Rep* 5: 16524

Vitriol EA, Zheng JQ (2012) Growth cone travel in space and time: the cellular ensemble of cytoskeleton, adhesion, and membrane. *Neuron* 73: 1068 – 1081

Wang W, Zhu JZ, Chang KT, Min KT (2012) DSCR1 interacts with FMRP and is required for spine morphogenesis and local protein synthesis. *EMBO J* 31: 3655 – 3666

Wang W, Rai A, Hur EM, Smilansky Z, Chang KT, Min KT (2016) DSCR1 is required for both axonal growth cone extension and steering. *J Cell Biol* 213: 451 – 462

Weingarten-Gabbay S, Elias-Kirma S, Nir R, Gritsenko AA, Stern-Ginossar N, Yakhini Z, Weinberger A, Segal E (2016) Comparative genetics. Systematic discovery of cap-independent translation sequences in human and viral genomes. *Science* 351: aad4939

Xue S, Tian S, Fujii K, Kladwang W, Das R, Barna M (2015) RNA regulons in Hox 5′ UTRs confer ribosome specificity to gene regulation. *Nature* 517: 33 – 38

Yam PT, Langlois SD, Morin S, Charron F (2009) Sonic hedgehog guides axons through a noncanonical, Src-family-kinase-dependent signaling pathway. *Neuron* 62: 349 – 362

Yeh SH, Yang WB, Gean PW, Hsu CY, Tseng JT, Su TP, Chang WC, Hung JJ (2011) Translational and transcriptional control of Sp1 against ischaemia through a hydrogen peroxide-activated internal ribosomal entry site pathway. *Nucleic Acids Res* 39: 5412 – 5423

Yoon BC, Zivraj KH, Strochlic L, Holt CE (2012) 14-3-3 proteins regulate retinal axon growth by modulating ADF/cofilin activity. *Dev Neurobiol* 72: 600 – 614

Zhang J, Roberts R, Rakotondrafara AM (2015) The role of the 5′ untranslated regions of Potyviridae in translation. *Virus Res* 206: 74 – 81

Zuker M (2003) Mfold web server for nucleic acid folding and hybridization prediction. *Nucleic Acids Res* 31: 3406 – 3415